

# Investigation of the Impact of Hydrolytically Cleavable Groups on the Stability of Poly(ethylene glycol) Based Hydrogels Cross-Linked via the Inverse Electron Demand Diels–Alder (iEDDA) Reaction

Christian E. Ziegler, Moritz Graf, Makoto Nagaoka, and Achim M. Goepferich\*

Eight-armed poly(ethylene glycol) (PEG) hydrogels cross-linked via inverse electron demand Diels–Alder reaction between norbornene and tetrazine groups are promising materials for long-term protein delivery. While a controlled release over 265 days is achieved for 15% w/v hydrogels in the previous study, the material shows high stability over 500 days despite having cleavable ester linkages between the PEG macromonomers and their functionalities. In this study, the hydrolyzable ester linkers in the PEG–norbornene precursor structure are exchanged to reduce the degradation time. To this end, 3,6-epoxy-1,2,3,6-tetrahydrophthalimide, phenyl carbamate, carbonate ester, and phenyl carbonate ester are introduced as degradable functional groups. Oscillatory shear experiments reveal that they are not affected the in situ gelation. All hydrogel types have gel points of less than 20 s even at a low polymer concentration of 5% w/v. Hydrogels with varying polymer concentrations have similar mesh sizes, all of which fell in the range of 4–12 nm. The inclusion of phenyl carbonate ester accelerates degradation considerably, with complete dissolution of 15% w/v hydrogels after 302 days of incubation in phosphate buffer (pH 7.4). Controlled release of 150 kDa fluorescein isothiocyanate-dextran over a period of at least 150 days is achieved with 15% w/v hydrogels.

less invasive procedure as compared to implantation, which decreases cost and improves patient compliance.<sup>[1–3]</sup> One way to achieve in situ gelation in delivery systems is the formation of covalent bonds between prefunctionalized hydrogel precursors by using chemical cross-linking.<sup>[2]</sup> To improve the material's potential for medical use, it is of utmost importance that these delivery systems do not have to be removed by explantation at the end of the therapy, but rather degrade into water-soluble products leading to polymer erosion and complete hydrogel dissolution. While degradation refers to the actual bond cleavage reaction, erosion designates the loss of mass from the polymer matrix.<sup>[4]</sup> For complete hydrogel erosion of covalently cross-linked hydrogels, there are two common degradation mechanisms. A simple approach is using cross-linking reactions of kinetically reversible nature.<sup>[5]</sup> These cross-links are cleaved by the removal of educts from the reaction equilibrium leading to degradation of the hydrogel network. For example, the degradation mechanism of hydrogels cross-


linked via Diels–Alder (DA) reaction between furan and maleimide relies on the hydrolysis of maleimide groups to non-reactive maleamic acid.<sup>[6,7]</sup> However, the DA reaction is not ideal for in situ gelation due to its slow reaction kinetics.<sup>[8–10]</sup> Further examples of biodegradable materials are systems cross-linked via Schiff base reactions such as imines and their derivatives including hydrazones and oximes.<sup>[11,12]</sup> Unfortunately, the hydrogel formation via Schiff base reactions poses a high risk for off-target reactions with cargo or molecules at the injection site by reactive groups, such as ketones and aldehydes.<sup>[13,14]</sup> This could additionally lead to structural damage to the embedded protein cargo or changes in the release kinetics.<sup>[15]</sup> Therefore, cross-linking reactions with higher reaction rate and selectivity are required.

A promising reaction is the inverse electron demand Diels–Alder (iEDDA) reaction between norbornene and tetrazine groups.<sup>[16]</sup> In addition to its fast reaction kinetics, the iEDDA reaction is bioorthogonal and highly efficient without using a catalyst or producing toxic byproducts.<sup>[17–19]</sup> The major drawback to the iEDDA reaction is that it is irreversible and, therefore, via

## 1. Introduction

In situ forming hydrogels are of great importance in the field of protein drug delivery because they can be injected in a much

C. E. Ziegler, M. Graf, M. Nagaoka, A. M. Goepferich  
Department of Pharmaceutical Technology  
Faculty of Chemistry and Pharmacy  
University of Regensburg  
93040 Regensburg, Germany  
E-mail: achim.goepferich@chemie.uni-regensburg.de

 The ORCID identification number(s) for the author(s) of this article can be found under <https://doi.org/10.1002/mabi.202200226>

© 2022 The Authors. Macromolecular Bioscience published by Wiley-VCH GmbH. This is an open access article under the terms of the Creative Commons Attribution-NonCommercial-NoDerivs License, which permits use and distribution in any medium, provided the original work is properly cited, the use is non-commercial and no modifications or adaptations are made.

DOI: 10.1002/mabi.202200226

iEDDA reaction cross-linked hydrogels require a different degradation pathway to make them degradable. Here, erosion can be achieved by incorporating hydrolytically, oxidatively, or enzymatically cleavable groups as predetermined breaking points into hydrogel precursors.<sup>[5]</sup> Polymers such as chitin, chitosan, dextran, and hyaluronic acid allow for enzymatic cleavage.<sup>[20–23]</sup> However, enzymatic degradation complicates the control and predictability of degradation because enzyme concentrations vary spatially within the tissue as well between individuals. When enzymes are added to the polymer matrix in an attempt to solve this problem, the loading capacity of the hydrogel is reduced, which is less than ideal.<sup>[24]</sup>

To overcome this drawback, passively hydrolyzable functional groups need to be incorporated into the polymer backbone. Prominent examples are ester, amide, carbamate, and carbonate ester groups that degrade at different rates.<sup>[25–28]</sup>

The goal of this study was to prepare poly(ethylene glycol) (PEG)-based hydrogels that degrade at different rates. For this purpose, 3,6-epoxy-1,2,3,6-tetrahydrophthalimide (ETPI), phenyl carbamate, carbonate ester, and phenyl carbonate ester were introduced into the norbornene-functionalized eight-armed PEG-hydrogel precursor as hydrolytically cleavable groups. Hydrogel formation was based on an iEDDA reaction of norbornene- and tetrazine-functionalized macromonomers. The gelation was evaluated by rheology to determine gel point and stiffness. Additionally, Young's modulus of compression (compressive modulus) was measured. The degradation time of the hydrogels was investigated as well as cytotoxicity and the mesh size. Finally, the hydrogels were loaded with fluorescein isothiocyanate-dextran (FITC-dextran) with a molecular weight of 150 kDa to determine the in vitro release kinetics.

## 2. Results and Discussion

### 2.1. Synthesis of PEG-Norbornene Derivatives with Different Biodegradable Linkers

To introduce various cleavable groups as predetermined degradation points into hydrogels (**Scheme 1**), different polymer functionalization mechanisms were used (**Scheme S1**, Supporting Information). For all the linkers synthesized for this work, end-group conversions ranging from 64% to 83% were achieved, which is satisfactory for cross-linking and comparable to other multiarmed PEG modifications.<sup>[29,30]</sup> The new biodegradable groups were synthesized into the PEG-norbornene precursor rather than the more reactive tetrazine groups to prevent hydrolysis and possible side reactions. Tetrazine-functionalized precursors were synthesized by esterification as previously published.<sup>[31]</sup> For the phenyl carbamate linker, a phenol was chosen as the leaving group. Carbamates consisting of phenols are chemically more labile than those made of aliphatic alcohols due to their lower  $pK_a$  values.<sup>[32,33]</sup> Using aliphatic alcohols as the leaving group for carbamate linkers would even lead to higher stability than the corresponding ester.<sup>[34]</sup> Similar to the carbamate linker, a phenol group was used as the leaving group for the phenyl carbonate ester linker to accelerate degradation. For the synthesis of norbornene functionalized precursors with the ETPI, phenyl carbamate, and phenyl carbonate linkers, amide groups were used that do not impact the degradation time due

to their high stability at physiological conditions.<sup>[35,36]</sup> In this way, comparison of the different linkers was possible. Overall, the syntheses presented here are a straightforward and cost-effective method to produce norbornene-functionalized multiarmed PEGs with different cleavable groups.

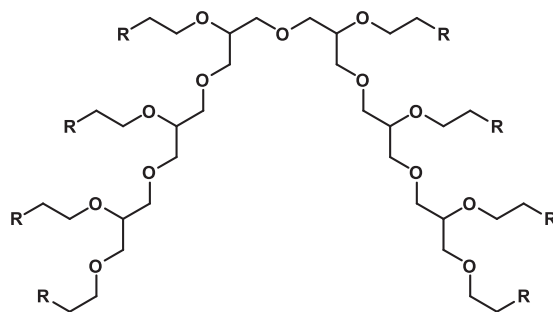
### 2.2. Gelation Time and Mechanical Properties

In situ forming systems are advantageous because they undergo gelation rapidly, thus avoiding material loss from the injection site. The gel formation rate can be characterized by the gel point, which is the time of the cross-over point of storage ( $G'$ ) and loss modulus ( $G''$ ). This point is where the transition from liquid-like to solid-like behavior occurs.<sup>[37]</sup> The gelation for each hydrogel was followed by oscillatory shear experiments.

**Figure 1** shows the rheograms of 5% w/v hydrogels with different degradable linkers. A very fast increase of  $G'$  ending in a plateau can be seen for all hydrogels. Gel points (**Figure 2**) of  $16.6 \pm 0.6$  s (ETPI linker),  $9.9 \pm 6.0$  s (phenyl carbamate linker),  $12.2 \pm 8.7$  s (carbonate ester linker), and  $5.9 \pm 3.8$  s (phenyl carbonate ester linker) were found, indicating very rapid in situ gelation already for a low polymer concentration of 5% w/v. Even though differences in the gelation time were not found to be significant for the ETPI linker, lower end-group conversion of the macromonomers could explain the increased gelation time for that linker.

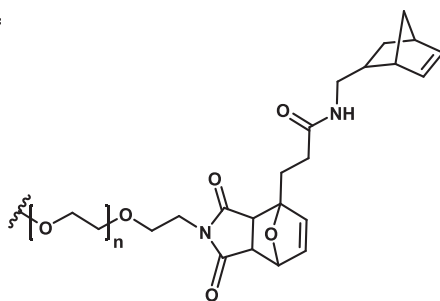
In addition to the gel point determination, rheology was used to measure the stiffness of the hydrogels after 30 min, when gelation was considered complete (**Figure 4A**). The absolute value of the complex shear modulus of hydrogels with the ETPI linker was found to be the significantly highest ( $2.7 \pm 0.2$  kPa). ETPI is the DA adduct between furan and maleimide. Since this DA adduct contains a norbornene derivative (7-oxanorbornene), it is possible that tetrazine reacts with the additional norbornene derivative as well as the unmodified norbornene groups. Previously, it was shown that tetrazine-functionalized 8armPEGs formed hydrogels with ETPI-functionalized 8armPEGs.<sup>[31]</sup> To check if tetrazine groups reacted with the incorporated ETPI linker,  $^1\text{H}$  NMR spectroscopy was used. An aqueous mixture of 8armPEG10k-ETPI-Nb and 8armPEG10k-Tz would make a highly cross-linked hydrogel, which could not have been investigated with classical  $^1\text{H}$  NMR spectroscopy. Therefore, we used linear tetrazine-functionalized methoxy PEG with a molecular weight of 5 kDa (mPEG5k-Tz) instead of 8armPEG10k-Tz so that the reaction products stayed in solution after polymerization and could be detected by  $^1\text{H}$  NMR spectroscopy. To determine the prevalence of the side reaction between tetrazine groups and

7-oxanorbornene, norbornene groups were used in excess to tetrazine groups. First, spectra of 8armPEG10k-ETPI-Nb and mPEG5k-Tz dissolved in  $\text{D}_2\text{O}$  with 2,2-dimethyl-2-silapentane-5-sulfonate sodium salt (DSS) as internal standard were recorded (**Figure 3A,B**). To maintain the same norbornene and DSS concentrations, solid mPEG5k-Tz was added to the NMR tube containing 8armPEG10k-ETPI-Nb. After incubating at  $37^\circ\text{C}$  for 1 h, the spectrum of the formed product was measured (**Figure 3C**). The disappearance of signal d indicated the complete consumption of tetrazine. The peaks at 6.63, 6.50, and 6.34 ppm represented the protons of the alkene bond in 7-oxanorbornene in the

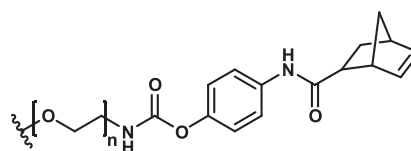


hexaglycerol core of 8armPEG10k

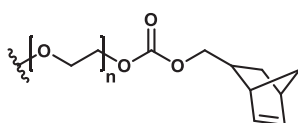
R =



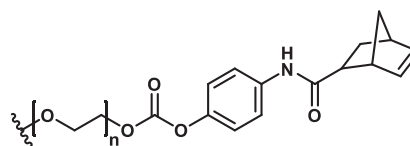
8armPEG10k-ETPI-Nb



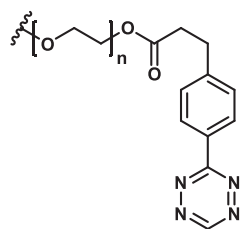
8armPEG10k-phenyl carbamate-Nb



8armPEG10k-carbonate-Nb



8armPEG10k-phenyl carbonate-Nb



8armPEG10k-Tz

**Scheme 1.** Chemical structures of tetrazine-functionalized eight-armed PEG with a molecular mass of 10 kDa (8armPEG10k-Tz) and norbornene-functionalized eight-armed PEG with a molecular mass of 10 kDa with ETPI (8armPEG10k-ETPI-Nb), phenyl carbamate (8armPEG10k-phenyl carbamate-Nb), carbonate ester (8armPEG10k-carbonate-Nb), and phenyl carbonate ester (8armPEG10k-phenyl carbonate-Nb) linkers. For simplification, only one isoform of the norbornene position is shown.

exo and endo positions (signal b). The protons at position c appeared as three peaks at 6.24 and 6.15 (endo) and 5.95 ppm (exo). Using the ratio of tetrazine to norbornene groups and integrating the peaks of the functional groups related to the internal standard, it was possible to calculate the percentage of groups that had reacted. Besides the decrease of the proton peak for the alkene bond at position c, the peaks of the protons at positions a and b decreased, indicating a side reaction of tetrazine with the ETPI linker. 82.5% of the unmodified norbornene and 17.5% of the 7-oxanorbornene were found to react with tetrazine groups.

These findings suggested that there are twice as many norbornene derivative groups present compared to tetrazine groups. This increases the likelihood for a tetrazine group to find a cross-linking counterpart for hydrogel formation. Consequently, the number of elastically active chains increases, giving the product a higher stiffness compared to systems with equimolar amounts of tetrazine and norbornene. No significant difference in stiffness was obtained for hydrogels containing phenyl carbamate ( $1.7 \pm 0.4$  kPa) or carbonate ester ( $1.8 \pm 0.2$  kPa) as cleavable linkers (Figure 4A). The significantly lowest stiffness was found for the

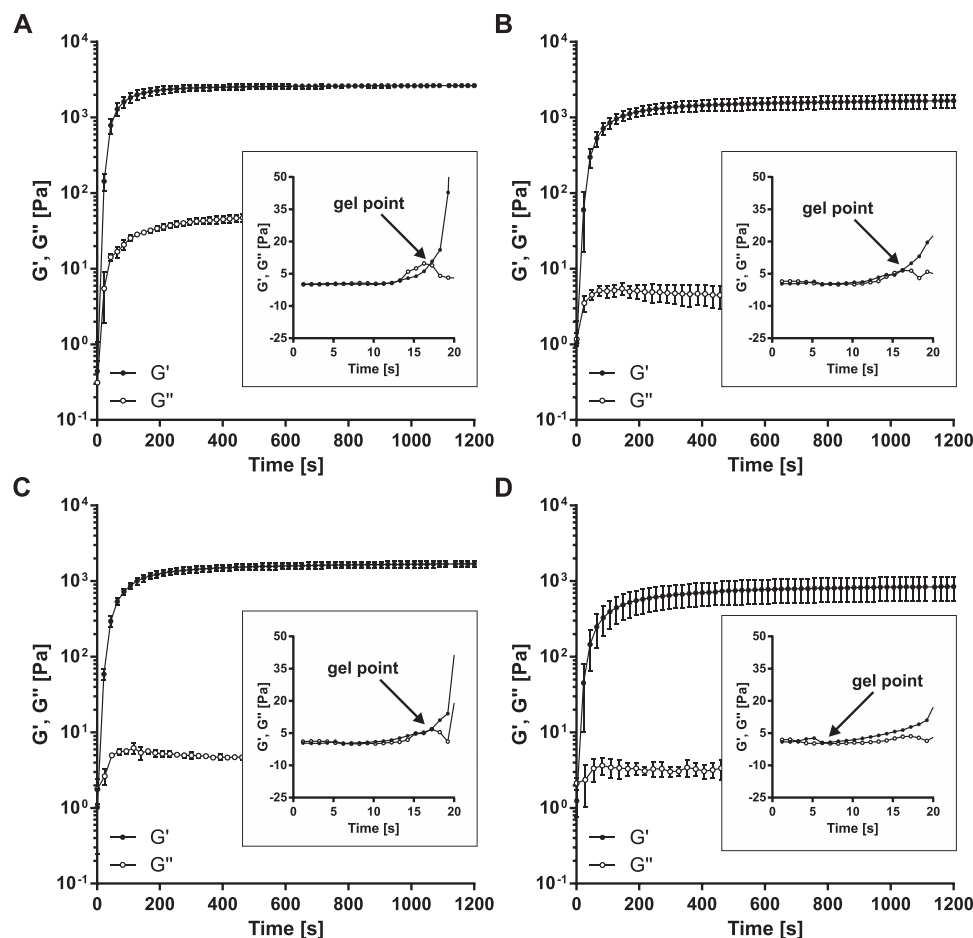


**Figure 1.** Rheograms of 5% w/v 8armPEG10k-hydrogels with ETPI linker A), phenyl carbamate linker B), carbonate ester linker C), and phenyl carbonate ester linker D) with insets showing the gel points of one representative hydrogel for each type. Storage ( $G'$ ) and loss modulus ( $G''$ ) were determined over time at 37 °C. All experiments were carried out at an oscillation frequency of 1.0 Hz using a 25 mm parallel plate geometry and a gap size of 500  $\mu\text{m}$ . The experiments were done in triplicate and the results are shown as means  $\pm$  standard deviations.

hydrogel with the phenyl carbonate ester linker ( $0.9 \pm 0.3$  kPa). This type of hydrogel is expected to degrade most quickly due to its high lability, which also has a negative impact on stiffness. Similar behavior was found for the compressive modulus (Figure 4B), which is defined as the ratio of compressive stress to compressive strain. Hydrogels with the phenyl carbonate ester linker showed the significantly lowest values ( $1.4 \pm 0.2$  kPa). Besides higher stiffness, the ETPI linker also had a significantly higher compressive modulus ( $9.0 \pm 0.4$  kPa) because of the increased number of binding partners for tetrazine groups. Hydrogels containing the phenyl carbamate ( $5.0 \pm 1.0$  kPa) and carbonate ester linkers ( $4.7 \pm 0.8$  kPa) did not show any significant differences in compressive modulus.

### 2.3. Cytotoxicity

Carbonate ester and phenyl carbamate groups are targets for nucleophilic groups, such as amines and alcohols. Contact with proteins can lead to interactions, including covalent bonds. Additionally, synthesis residues of educts such as phosgene and

its derivatives can cause toxicity.<sup>[38,39]</sup> To exclude toxicity of the synthesis residues, the formed hydrogel, and nonreacted macromonomers, cytocompatibility of all hydrogels consisting of different biodegradable linkers was assessed (Figure 5). For this, 15% w/v hydrogels were separately incubated in Eagle's minimum essential medium (EMEM) supplemented with 10% fetal calf serum (FCS) for 24 h. Afterward, the supernatants were added to mouse fibroblast L-929 cells and the 3-(4,5-Dimethylthiazol-2-yl)-2,5-diphenyltetrazolium bromide (MTT) assay was performed. For hydrogels with different biodegradable linkers, cell viabilities of  $98.2 \pm 4.1\%$  (ETPI),  $100.7 \pm 5.1\%$  (phenyl carbamate),  $96.2 \pm 4.9\%$  (carbonate ester), and  $89.1 \pm 4.2\%$  (phenyl carbonate ester) were found. Hydrogels containing the ETPI and phenyl carbamate linkers both had minimal impacts on viability. The higher stability imparted by the ETPI and phenyl carbamate linkers might have protected the cells from detrimental interactions and resulted in no toxicity. In contrast, carbonate ester and phenyl carbonate ester as biodegradable linker resulted in significant viability decreases. The reason for this becomes apparent upon examining the syntheses of 8armPEG10k-carbonate-Nb and 8armPEG10k-phenyl carbonate-

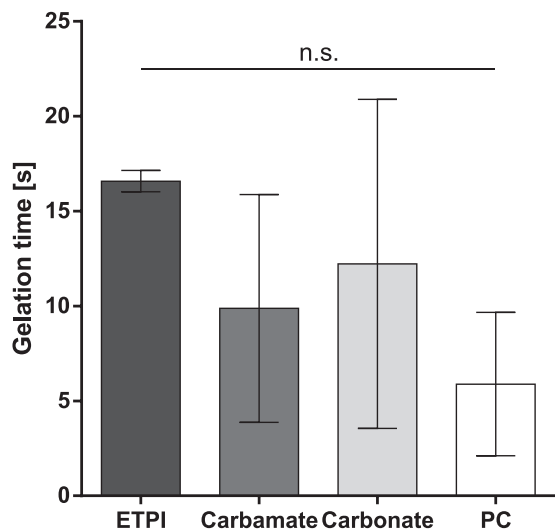


**Figure 2.** Gelation time of 5% w/v 8armPEG10k-hydrogels containing ETPI linker, phenyl carbamate linker (carbamate), carbonate ester linker, and phenyl carbonate ester linker (PC) at 37 °C. The experiments were done in triplicate and the results are shown as means ± standard deviations.

Nb, which included phosgene and its derivatives. Possible educt residues after purification could explain the observed effects on cell viability. Additionally, the phenyl carbonate ester linker is expected to degrade faster than the carbonate ester linker due to the incorporation of a phenyl elimination group. Therefore, nucleophilic residues from the cells can preferentially attack the electrophilic structure. In summary, all hydrogels exceeded the 70% threshold value of ISO 10993-5:2009 clearly. However, by using this cytocompatibility test only the toxicity of the synthesis residues, the formed hydrogel, and nonreacted macromonomers was investigated. For effects of the degradation products, an investigation over a prolonged time frame would be required. Additionally, in vivo biocompatibility tests are necessary for a full evaluation of toxicity.

#### 2.4. Swelling and Degradation Studies

The aim of this study was to investigate the influence of the different hydrolytically cleavable groups on the stability of 8armPEG10k-hydrogels. In contrast to former studies, the ester group of the PEG-norbornene precursor was replaced by a new cleavable linker, while the ester group of PEG-tetrazine was unchanged.<sup>[31]</sup> In this manner, we should be able to decrease the long degradation time of 8armPEG10k-hydrogels cross-linked via iEDDA reaction with two incorporated ester groups as designated breaking points (**Scheme 2**). The impact of the ester groups in the PEG-tetrazine precursor on the stability of the hydrogels was considered negligible since approximately the same amount of ester groups was present in all types of hydrogels.

To examine the stability of these hydrogels, swelling studies were performed. All hydrogels were placed in 50 mM phosphate buffer (pH 7.4) at 37 °C, and the development of the relative mass was followed over time. The degradation time was defined as the time for complete dissolution of the hydrogels. For each

linker, hydrogels were prepared with polymer concentrations of 5%, 10%, and 15% w/v to meet diverse application requirements (Figure S1, Supporting Information). To better see the difference in mass change, **Figure 6** shows the relative mass development of all hydrogels prepared with an overall polymer concentration of 5% w/v.

For ETPI and carbonate ester, we observed swelling behavior similar to that of hydrogels containing two ester groups. After a decrease in the relative mass due to syneresis and network contraction, the hydrogels started to take up water, leading to slow bulk degradation with simultaneous mass increase.<sup>[40,26]</sup> For 400 days, no mass decrease was seen, and no faster degradation was obtained with either of these linkers. Phenyl carbamate groups also led to a volume contraction followed by a larger mass increase. However, the hydrogel mass started to decrease after reaching a maximum at 175 days due to linker cleavage and erosion. After 409 days, the hydrogel matrix still eroded, and no faster degradation could be detected. In contrast, no mass increase could be found for hydrogels containing the phenyl carbonate ester linker. For this linker, the hydrogel eroded from beginning to complete erosion after 153 days. The phenyl carbonate ester linker degraded faster than the carbonate ester linker because of resonance stabilization in the phenyl leaving group. This degradation results in a diffusion of the free macromonomers from the hydrogels to the surrounding solution and mass loss starting immediately after incubation with buffer. Interestingly, hydrogels containing the phenyl carbonate ester linker were the only hydrogel type that showed differences in swelling behavior for higher polymer concentrations (Figure S1D, Supporting Information). After surface erosion over 109 days, the remaining matrix of the 10% and 15% w/v hydrogels started to gain mass. At this point for the 5% w/v hydrogels, most of the phenyl carbonate ester groups were already cleaved, preventing the hydrogel from swelling, and resulting in complete dissolution after 153 days. Only small differences in degradation time were detected for 10% and 15% w/v hydrogels. 15% w/v hydrogels completely dissolved after 309 days, whereas 10% w/v hydrogels were more stable and took 315 days to dissolve fully. We expected the more concentrated hydrogels to be more stable because 15% w/v hydrogels should have the largest number of elastically active chains and phenyl carbonate ester groups, which should take the longest to be completely degraded. This was already described for similar 8armPEG-hydrogels.<sup>[41,42]</sup> However, the 15% w/v hydrogels had the fastest gelation times, which caused them to have more irregularities compared to the 10% w/v hydrogels. Therefore, the 10% w/v hydrogels had more time to form a more homogeneous network during gelation, causing them to have similar stability to the 15% w/v hydrogels.

Since the cross-linking reaction is not assumed to occur quantitatively during gelation, unreacted norbornene, and tetrazine groups are present in the hydrogel. However, these free, unreacted functional groups do not allow for delayed cross-linking for reasons of low stability of hydrogen-substituted tetrazines in water.<sup>[43]</sup> Once the hydrogel is sufficiently degraded, which is considered to take several days, the free tetrazine groups would be fully hydrolyzed.

The degradation mechanism (**Scheme 3**) of carbamate and carbonate ester involves the nucleophilic attack of water and the formation of carbon dioxide.<sup>[44,45]</sup> In neutral milieu, a  $B_{AC}2$



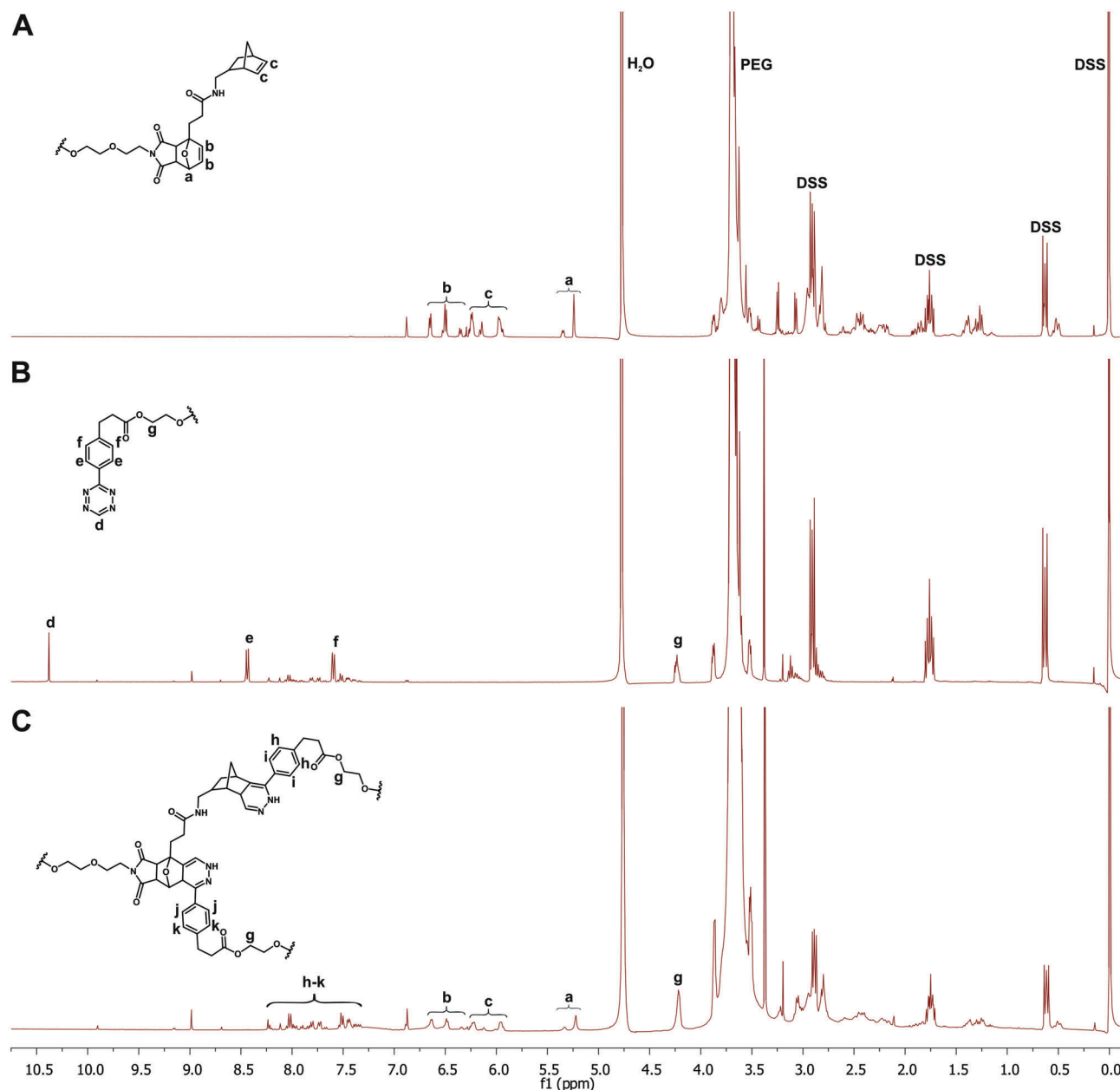


**Figure 3.** <sup>1</sup>H NMR spectra of 8armPEG10k-ETPI-Nb A), mPEG5k-Tz B), and the product between 8armPEG10k-ETPI-Nb and mPEG5k-Tz after reaction in D<sub>2</sub>O at 37 °C for 1 h C). All spectra were recorded in D<sub>2</sub>O with DSS as internal standard.

mechanism is advanced for the carbonate ester hydrolysis.<sup>[46]</sup> Thereby, carbonate ester groups can show higher stability than ester groups.<sup>[44]</sup> On the other hand, introducing a resonance-stabilized leaving group results in lower stability as seen for the phenyl carbonate ester linkers. Carbamates hydrolyze via an E1cB elimination reaction mechanism.<sup>[47,48]</sup> An unstable isocyanate intermediate is formed, which reacts with water to form an amine and carbon dioxide. Again, a resonance-stabilized leaving group increases the degradation rate. For the ETPI linker, the hydrolysis of free maleimide groups removes maleimides from the reaction equilibrium, enhancing the retro-Diels–Alder reaction and degradation of the hydrogel. Previously, we showed that 5% w/v

8armPEG40k-hydrogels cross-linked via DA reaction containing one ETPI group per cross-link dissolved after ≈10 days, whereas 5% w/v 8armPEG40k-hydrogels containing two ester groups per cross-link were completely dissolved after about 60 days.<sup>[42,35]</sup> Therefore, we assumed a significant difference in degradation time. However, no faster degradation could be found. The reason for this is that ETPI linkers are a target for tetrazine groups reacting as described above (Figure 3C). These additional cross-links are not subject to hydrolysis, making the system more stable. Hence, the ETPI linker is not a suitable hydrolyzable functional group for degradable hydrogel synthesis cross-linked via iEDDA reaction. However, for cross-linking reactions such as Schiff base

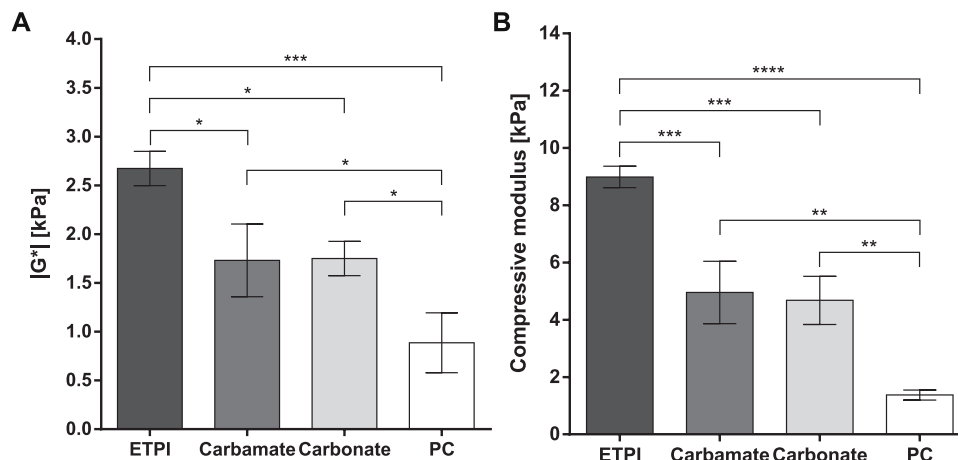


**Figure 4.** Stiffness represented by the absolute value of the complex shear modulus ( $|G^*|$ ) after 30 min of gelation time for 5% w/v 8armPEG10k-hydrogels containing ETPI linker, phenyl carbamate linker (carbamate), carbonate ester linker, and phenyl carbonate ester linker (PC) A). The compressive modulus of 5% w/v 8armPEG10k-hydrogels containing ETPI linker, phenyl carbamate linker (carbamate), carbonate ester linker, and phenyl carbonate ester linker (PC) B). The experiments were done in triplicate and the results are shown as means  $\pm$  standard deviations. Statistical significance was assessed using one-way ANOVA. Post hoc analysis was determined by Tukey's test. Levels of statistical significance are indicated as  $*p \leq 0.05$ ,  $**p \leq 0.001$ ,  $***p \leq 0.001$ , and  $****p \leq 0.0001$ .

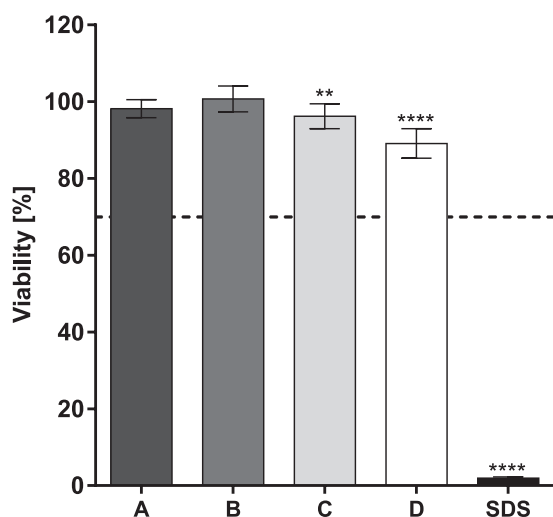


**Figure 5.** Viability of L-929 cells after incubation with extracts from 15% w/v 8armPEG-iEDDA hydrogels that contained ETPI A), phenyl carbamate B), carbonate ester C), and phenyl carbonate ester D) as biodegradable linkers. 0.1% w/v sodium dodecyl sulfate (SDS) in cell medium served as negative control. The dotted line at 70% cell viability indicates the threshold for cytocompatibility. All hydrogels passed this threshold showing no cytotoxicity. Statistical significance was assessed relative to the positive control, which was pure medium. The experiments were done with at least six replicates and the results are shown as means  $\pm$  standard deviations. Statistical significance was assessed using one-way ANOVA. Post hoc analysis was determined by Tukey's test. Levels of statistical significance are indicated as  $**p \leq 0.01$  and  $****p \leq 0.0001$ .

formation or condensation reactions with no reactivity toward norbornene functionalities, the ETPI linker could be used.

In summary, only the incorporation of the phenyl carbonate ester linker into the 8armPEG10-Nb precursor led to faster degradation compared to our former hydrogels with two ester groups, which dissolved after 438 days. Additionally, further studies on

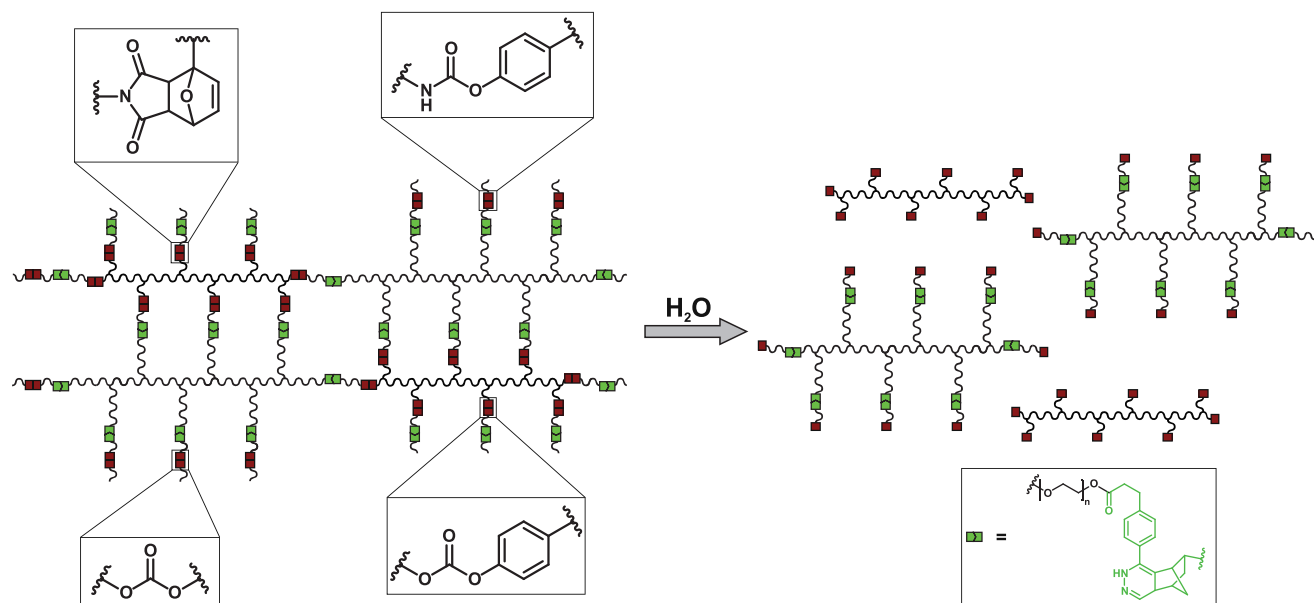
the degradation and erosion at different pH values are required to shed light on the use of these hydrogels in vivo.

## 2.5. Mesh Size and FITC-Dextran Release

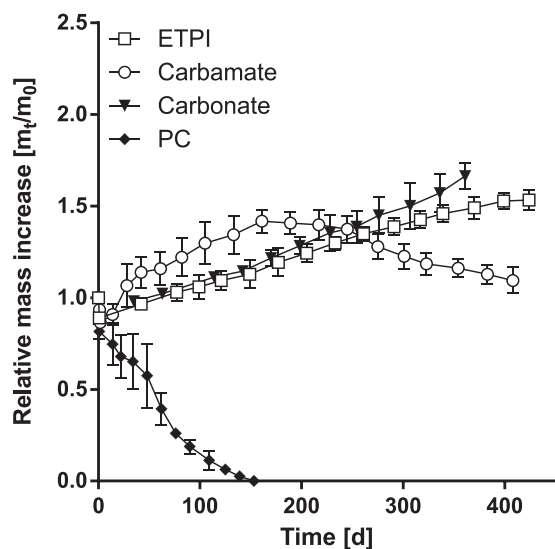
After thoroughly characterizing the hydrogels synthesized with different biodegradable linkers, FITC-dextran release from the hydrogels was examined. First, the mesh sizes of hydrogels made with different polymer concentrations were determined. In addition to degradation behavior and drug diffusivity, the mesh size of a hydrogel is a pivotal factor in drug release kinetics.<sup>[49-51]</sup> It is necessary to choose a hydrogel with a mesh size in the range of the hydrodynamic diameter of the drug for controlled release over time without delay. The mesh sizes were compared to 8armPEG10k-hydrogels cross-linked via iEDDA reaction with two cleavable ester groups. Since for this hydrogel type, a controlled release of FITC-dextran over a time of more than 250 days could be achieved,<sup>[31]</sup> the mesh sizes of the hydrogels with the new degradable linkers should be in the same range.

Table 1 shows the average mesh sizes of all hydrogels at three different polymer concentrations. For all four biodegradable linkers, mesh sizes comparable to our previously published values of iEDDA-hydrogels were found.<sup>[31]</sup> For the successful release of FITC-dextran with a hydrodynamic radius of 9.0 nm<sup>[52]</sup> from 8armPEG10k-hydrogels, a polymer concentration of 15% w/v with an average mesh size of  $4.1 \pm 0.2$  nm was used. Therefore, the same polymer concentration was chosen for the release experiments with the biodegradable linkers, with mesh size values of  $4.4 \pm 0.6$  nm (ETPI),  $4.6 \pm 0.1$  nm (phenyl carbamate),  $4.2 \pm 0.0$  nm (carbonate ester), and  $4.9 \pm 0.5$  nm (phenyl carbonate ester). Differences in the mesh sizes of the various 15% w/v 8armPEG10k-hydrogels were not significant.

The release of 150 kDa FITC-dextran from all hydrogel types with a polymer concentration of 15% w/v was examined to investigate the influence of the linker on the release kinetics. FITC-



**Scheme 2.** Degradation of 8armPEG10k-hydrogels due to the hydrolytically cleavage of different linkers.



**Figure 6.** Swelling and degradation of 5% w/v 8armPEG10k-hydrogels containing ETPI, phenyl carbamate, carbonate ester, and phenyl carbonate ester (PC) as hydrolytically cleavable groups in 50 mM phosphate buffer (pH 7.4) at 37 °C. The experiments were done in triplicate and the results are shown as means  $\pm$  standard deviations.

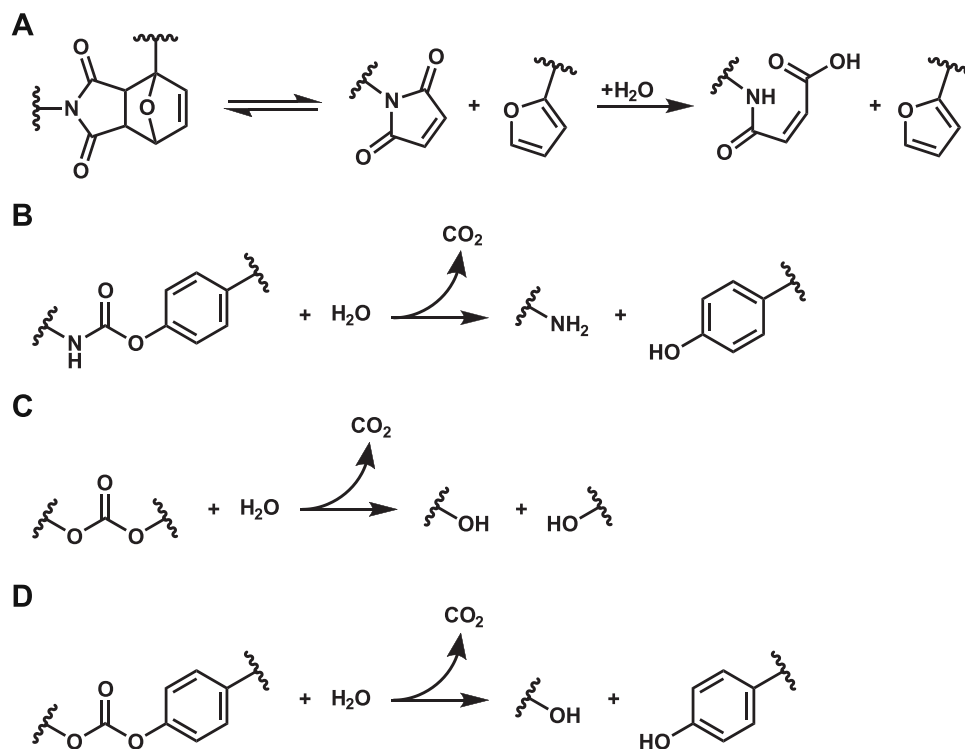
dextran was chosen as a model substance because of its high stability in phosphate buffer.<sup>[53]</sup> **Figure 7** shows the release kinetics of FITC-dextran from the various hydrogels. For all hydrogels, controlled release over 150 days can be seen. The initial release varied from about 20% for the ETPI and carbonate ester linkers to  $\approx$ 13% for the phenyl carbamate and phenyl carbonate ester linkers. After the initial release, the model substance was released in a fast manner over 20 days for the ETPI and carbonate ester linkers. Subsequently, FITC-dextran was released continuously until

the experiment was stopped. Thereby, FITC-dextran was released faster from hydrogels containing the ETPI linker.

Phenyl carbamate or phenyl carbonate ester linkers led to a slower initial release of the model substance followed by continuous release over the respective time frame. Subsequently, hydrogels with the phenyl carbonate ester linker released the FITC-dextran more quickly because of their lower stability, which resulted in faster mesh size increases and less hindered diffusion from the network. Interestingly, the amount released over the first 90 days was lower for the phenyl carbamate and phenyl carbonate ester linkers compared to the ETPI and carbonate ester linkers. Hydrogels with phenyl carbamate and phenyl carbonate ester share different swelling kinetics compared to the other hydrogels. Differences in swelling behavior most likely affect the release kinetics because of their influence on the network density. In a recent study, we showed that it is possible to prepare a controlled release system based on 8armPEGk-precursors cross-linked via the iEDDA reaction between norbornene and tetrazine groups.<sup>[31]</sup> The model substance FITC-dextran with a molecular weight of 150 kDa was released over an extended time of 265 days. In contrast to other long-term release approaches that rely on the inclusion of additional substances such as micro- and nanoparticles<sup>[54,55]</sup> or incorporation of drug affine groups into the hydrogel backbone<sup>[56–58]</sup> the high stability and slow swelling behavior of the hydrogel itself were exploited. This is advantageous as no additional excipients are required, and arbitrary therapeutic proteins can be embedded in the hydrogel network without concern for their affinity. However, an overly long release time can cause challenges regarding protein stability, such as denaturation and activity loss.

To shorten the release time, four different degradable groups were incorporated in the hydrogel backbone. Only the phenyl carbonate ester linker was found to degrade faster than the ester groups in our previous study.





**Scheme 3.** Degradation mechanism of ETPI A), phenyl carbamate B), carbonate ester C), and phenyl carbonate ester linker D) in water.

**Table 1.** Average mesh size ( $\xi$ ) of 8armPEG10k-hydrogels consisting of different biodegradable linkers. All hydrogel types were prepared with polymer concentrations of 5%, 10%, and 15% w/v. The experiments were done in triplicate and the results are shown as means  $\pm$  standard deviations.

Linker	Concentration [% w/v]	$\xi$ [nm]
ETPI	5	11.4 $\pm$ 0.6
	10	6.2 $\pm$ 0.4
	15	4.4 $\pm$ 0.6
Phenyl carbamate	5	11.9 $\pm$ 1.0
	10	6.8 $\pm$ 0.4
	15	4.6 $\pm$ 0.1
Carbonate ester	5	10.6 $\pm$ 0.3
	10	5.8 $\pm$ 0.1
	15	4.2 $\pm$ 0.0
Phenyl carbonate ester	5	10.2 $\pm$ 1.2
	10	7.4 $\pm$ 0.3
	15	4.9 $\pm$ 0.5

The release experiments showed that the hydrogels with different hydrolyzable linkers were able to release a model substance with hydrodynamic diameter similar to common antibodies in a controlled manner over an extended time. These systems could be used to create drug depots for biologics like bevacizumab, ranibizumab, and trastuzumab to treat diseases such as early-stage breast cancer or age-related macular degeneration over long treatment periods, while avoiding frequent injections and leading to higher patient compliance.<sup>[59,60]</sup>

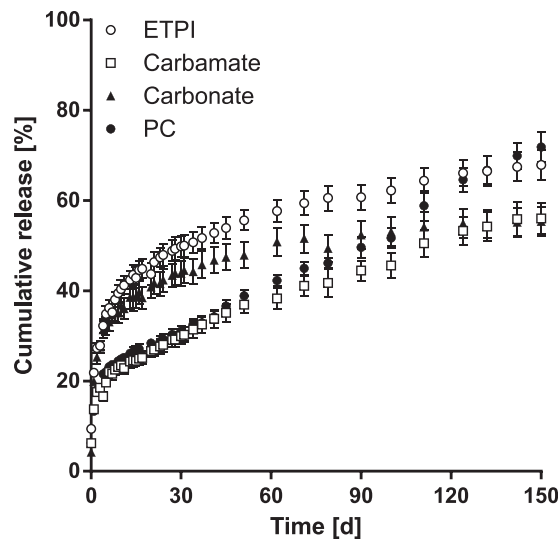


**Figure 7.** Release of FITC-dextran with a molecular weight of 150 kDa from 15% w/v 8armPEG10k-hydrogels containing ETPI linker, phenyl carbamate linker, carbonate ester linker, and phenyl carbonate ester linker (PC). The release experiments were carried out in 50 mM phosphate buffer (pH 7.4) at 37 °C. The experiments were done in triplicate and the results are shown as means  $\pm$  standard deviations.

### 3. Conclusion

The introduction of different hydrolyzable groups as predetermined breaking points into multiarmed PEG-hydrogels led to

a tunable degradation time. While hydrogels consisting of carbonate ester linkers prepared from alcohols did not show faster degradation than the previously published hydrogels with ester groups, changing the leaving group from an alcohol to a phenol decreased the stability and accelerated hydrogel degradation. Furthermore, all of the biodegradable linkers we tested still formed hydrogels with rapid in situ gelation processes and consistent mesh sizes. Additionally, phenyl carbamate groups caused a change in swelling behavior. All hydrogels achieved controlled release of FITC-dextran for more than 150 days regardless of the type of hydrolyzable linker. The hydrogel syntheses presented here are promising methods for the creation of materials tailored to many diverse biomedical applications.

## 4. Experimental Section

**Materials:** 4-Aminophenol, anhydrous acetonitrile, deuterated chloroform, anhydrous dichloromethane (DCM), *N,N'*-dicyclohexylcarbodiimide, diisopropyl azodicarboxylate, anhydrous *N,N'*-dimethylformamide (DMF), DSS, deuterated dimethyl sulfoxide, *N,N'*-disuccinimidyl carbonate (DSC), EMEM, absolute ethanol, anhydrous ethyl acetate (EtOAc), FCS, FITC-dextran with a molecular mass of 150 kDa, 3-(2-furyl)propanoic acid, glacial acetic acid, hexane, hydrazine monohydrate, *N*-methoxycarbonylmaleimide, 5-norbornenecarboxylic acid (mixture of endo and exo), protein LoBind Eppendorf tubes, pyridine, QuantiPro BCA Assay Kit, sodium bicarbonate, sulfur, anhydrous tetrahydrofuran (THF), triethylamine (TEA), and triphosgene were acquired from Sigma-Aldrich (Taufkirchen, Germany). 8armPEG10k and mPEG5k were purchased from JenKem Technology (Allen, TX) and functionalized with amine, maleimide, and tetrazine groups as previously described.<sup>[61,30,31]</sup> 4-Dimethylaminopyridine (DMAP), phthalimide, and anhydrous sodium sulfate were received from Acros Organics (Geel, Belgium). Cyclohexane p.a. and DCM p.a. were obtained from Fisher Chemical (Loughborough, UK). Diethyl ether (technical grade) was purchased from Jäcklechemie (Nuremberg, Germany). *O*-(Benzotriazol-1-yl)-*N,N,N',N'*-tetramethyluronium-hexafluorophosphate (HBTU), citric acid monohydrate, hydrochloric acid (HCL), silica gel 60 (0.063–0.200 mm), sodium azide, sodium dihydrogen phosphate monohydrate, sodium hydroxide, sodium nitrite, thionyl chloride, and triphenylphosphine were purchased from Merck KGaA (Darmstadt, Germany). 5-Norbornene-2-methanol and 5-norbornene-2-methylamine were obtained from TCI Chemicals (Eschborn, Germany). 3-(4-Cyanophenyl)-propionic acid was obtained from abcr GmbH (Karlsruhe, Germany). Tetramethylethylenediamine was purchased from Carl Roth GmbH & Co. KG (Karlsruhe, Germany). MTT and SDS were received from PanReac AppliChem (Darmstadt, Germany). Ethanol was purchased from Labochem international (Heidelberg, Germany). Gibco Dulbecco's phosphate-buffered saline was acquired from Life Technologies (Darmstadt, Germany). Mouse fibroblast cells were a kind gift from the group of Prof. Armin Buschauer (University of Regensburg). Purified water was freshly prepared using a Milli-Q water purification system from Millipore (Schwalbach, Germany).

**4.0.0.1. <sup>1</sup>H and <sup>13</sup>C NMR Spectroscopy:** <sup>1</sup>H and <sup>13</sup>C NMR spectra were recorded using a Bruker Avance III 400 spectrometer (Bruker BioSpin GmbH, Rheinstetten, Germany). To calculate end-group conversion, the integral of the alkene proton peak of norbornene groups was compared to the integral of the PEG backbone peak at δ3.75–3.40 ppm.

**Synthesis of *N*-(bicyclo[2.2.1]hept-5-en-2-yl)methyl-3-(furan-2-yl)propanamide:** 3-(2-Furyl)-propanoic acid chloride was synthesized as previously described.<sup>[62]</sup> Amidation was performed using a modified version of the synthesis described in literature.<sup>[63]</sup> In brief, 3-(2-furyl)-propanoic acid chloride was dissolved in anhydrous THF (10 mL), and the solution was added to a stirred solution of 5-norbornene-2-methylamine and pyridine (1.1 eq) in anhydrous THF (15 mL) at 0 °C. Afterward, the mixture was warmed to 20 °C, at which it was maintained overnight. It

was then diluted with water (60 mL), extracted with EtOAc (3 × 30 mL) and dried over anhydrous sodium sulfate. The solution was concentrated by rotary evaporation. The crude product was purified by column chromatography. The yield was 70%.

**Synthesis of 8armPEG10k-ETPI-Nb (Scheme 1):** A mixture of 8armPEG10k-maleimide and *N*-(bicyclo[2.2.1]hept-5-en-2-yl)methyl-3-(furan-2-yl)propanamide in anhydrous EtOAc (10 mL) was stirred for 3 days at room temperature. Afterward, the product was precipitated in cold diethyl ether three times. The residue was dissolved in EtOAc and extracted with water four times. The aqueous layer was washed twice with diethyl ether and filtered. Subsequently, the product was extracted with DCM three times, and the organic phase was dried over sodium sulfate. The solvent was concentrated, and the product was precipitated several times with cold diethyl ether. Finally, the product was dried under vacuum. The yield was 98%, and the degree of end-group conversion was 64%, as determined by <sup>1</sup>H NMR spectroscopy.

**Synthesis of *N*-(4-hydroxyphenyl)bicyclo[2.2.1]hept-5-ene-2-carboxamide:** 5-Norbornene-2-carboxylic acid, 4-aminophenol, and TEA were dissolved in anhydrous DMF. HBTU was dissolved in anhydrous DMF. Both solutions were combined and stirred for 2 h at room temperature under argon atmosphere. Subsequently, the solvent was evaporated. The residue was dissolved in EtOAc, washed with HCl solution (pH 3), brine and water, and dried over sodium sulfate. After evaporation of the solvent, the product was further purified by column chromatography. The yield was 96%.

**Synthesis of 4-(bicyclo[2.2.1]hept-5-ene-2-carboxamido)phenyl (2,5-dioxopyrrolidin-1-yl) carbonate:** *N*-(4-Hydroxyphenyl)bicyclo[2.2.1]hept-5-ene-2-carboxamide was dissolved in anhydrous acetonitrile, and pyridine and DSC were added. The solution was stirred for 18 h at room temperature. Afterward, the solvent was concentrated, DCM was added, and the formed solid was filtered off. The solvent was completely evaporated, and the residue was taken up in EtOAc to give a suspension. The organic phase was washed with 5% citric acid twice and brine once and dried over sodium sulfate. The solvent was evaporated and, finally, vacuum dried. The yield was 80%.

**Synthesis of 8armPEG10k-phenyl carbamate-Nb (Scheme 1):** 8armPEG10k-NH<sub>2</sub> and 4-(bicyclo[2.2.1]hept-5-ene-2-carboxamido)phenyl (2,5-dioxopyrrolidin-1-yl) carbonate were dissolved separately in anhydrous acetonitrile. The two solutions were combined, and TEA was added. The solution was stirred for 18 h under argon atmosphere. Afterward, the precipitate was filtered off and the solvent was evaporated. The residue was taken up in DCM and the suspension was centrifuged several times to separate the precipitate. Subsequently, the product was crystallized with diethyl ether. The crystallization step was repeated several times. The product was finally vacuum dried. The yield was 71% and the degree of end-group conversion was 83%, as determined by <sup>1</sup>H NMR spectroscopy.

**Synthesis of 8armPEG10k-carbonate-Nb (Scheme 1):** 5-Norbornene-2-methanol, triphosgene, and TEA were dissolved in anhydrous DCM at 0 °C and stirred for 3 h. A solution of 8armPEG10k and DMAP in anhydrous DCM was added, and the combined solution was warmed up to room temperature. The solution was stirred 2 days. Then, the solvent was evaporated, and the residue was dissolved in anhydrous THF. Subsequently, the suspension was centrifuged, and the precipitate was removed. This step was repeated. Afterward, the product was precipitated with cold cyclohexane several times and dried under vacuum. The yield was 55% and the degree of end-group conversion was 79%, as determined by <sup>1</sup>H NMR spectroscopy.

**Synthesis of 8armPEG10k-phenyl carbonate-Nb (Scheme 1):** *N*-(4-Hydroxyphenyl)bicyclo[2.2.1]hept-5-ene-2-carboxamide, triphosgene, and TEA were dissolved in anhydrous DCM at 0 °C and stirred for 3 h. A solution of 8armPEG10k and DMAP in anhydrous DCM was added and the combined solution was warmed up to room temperature. The solution was stirred for 2 days. Then, the solvent was evaporated. The residue was taken up in anhydrous THF. Subsequently, the suspension was centrifuged, and the precipitate was removed. This step was repeated. Afterward, the product was precipitated with cold cyclohexane several times and dried under vacuum. The yield was 98% and the degree of end-group conversion was 71%, as determined by <sup>1</sup>H NMR spectroscopy.

**Hydrogel Preparation:** For hydrogel preparation, norbornene- and tetrazine-functionalized 8armPEG10k-precursors (Scheme 1) were dissolved with an equal molar amount of tetrazine and norbornene groups in water. After combining both solutions, 200  $\mu\text{L}$  were transferred into cylindrical glass molds. The solution was allowed to gel for 1 h at 37  $^{\circ}\text{C}$ . The overall polymer concentrations were 5%, 10%, and 15% w/v.

**Hydrogel Characterization:** Oscillatory shear experiments were performed on a Malvern Kinexus Lab+ rheometer (Malvern, Kassel, Germany) at 37  $^{\circ}\text{C}$  with 25 mm parallel plate geometry, gap size of 500  $\mu\text{m}$ , constant oscillation frequency of 1.0 Hz, and a strain of 1%. Storage ( $G'$ ), loss modulus ( $G''$ ), and complex shear modulus ( $G^*$ ) were recorded over time. The cross over point of  $G'$  and  $G''$  was regarded as the gel point. The absolute values of the complex shear modulus ( $|G^*|$ ) were determined after 30 min when polymerization was considered complete. Water evaporation was reduced by using a solvent trap. Only hydrogels with a polymer concentration of 5% w/v were analyzed because higher concentrations resulted in faster gelation, which complicated handling.

The determination of the average mesh size ( $\xi$ ) was carried out according to the equilibrium swelling theory.<sup>[64,28]</sup> The gel volumes after cross-linking ( $V_{\text{gc}}$ ) and after swelling ( $V_{\text{gs}}$ ) were determined using Archimedes' principle of buoyancy. With the PEG density taken as 1.12  $\text{g mL}^{-1}$ ,<sup>[30]</sup> the dry polymer volume ( $V_{\text{p}}$ ) was obtained after freeze-drying the hydrogels. Subsequently, the polymer fraction of the hydrogel after cross-linking ( $\nu_{2c} = V_{\text{p}}/V_{\text{gc}}$ ) and in swollen state ( $\nu_{2s} = V_{\text{p}}/V_{\text{gs}}$ ) were calculated. The number of moles of elastically active chains in the hydrogel network ( $\nu_e$ ) was calculated by means of a modified version of the Flory–Rehner equation<sup>[65–67]</sup>

$$\nu_e = -\frac{V_{\text{p}}}{V_1\nu_{2c}} \cdot \frac{[\ln(1 - \nu_{2s}) + \nu_{2s} + \chi_1\nu_{2s}^2]}{\left[\left(\frac{\nu_{2s}}{\nu_{2c}}\right)^{\frac{1}{3}} - \frac{2}{f}\left(\frac{\nu_{2s}}{\nu_{2c}}\right)\right]} \quad (1)$$

Parameters required for Equation (1) are the molar volume of solvent,  $V_1$ , (18  $\text{mL mol}^{-1}$  for water),<sup>[68]</sup> the Flory–Huggins interaction parameter of PEG in water,  $\chi_1$ , (0.426),<sup>[69]</sup> and the branching factor of the macromonomers,  $f$ , (eight for 8armPEG).  $\xi$  was calculated as suggested by Canal and Peppas<sup>[70]</sup>

$$\xi = \nu_{2s}^{-\frac{1}{3}} l \left(\frac{2m_{\text{p}}}{\nu_e M_r}\right)^{\frac{1}{2}} C_n^{\frac{1}{2}} \quad (2)$$

In Equation (2),  $l$  is the average bond length along the PEG backbone (0.146 nm),<sup>[71]</sup>  $m_{\text{p}}$  is the total mass of polymer in the hydrogel,  $M_r$  is the molecular mass of the PEG repeating unit (44  $\text{g mol}^{-1}$ ), and  $C_n$  is the Flory characteristic ratio (four for PEG).<sup>[71]</sup>

The compressive modulus was determined according to the literature.<sup>[31]</sup> In brief, 5% w/v 8armPEG10k-hydrogels with a volume of 200  $\mu\text{L}$  were prepared for all linkers as described above. The diameter and height of the hydrogels were measured. After casting the hydrogel cylinders on the lower plate of an Instron 5542 materials testing machine (Norwood, MA), the samples were compressed uniaxially at a speed of 1  $\text{mm min}^{-1}$ . Compressive force ( $N$ ) and compressive strain (%) were monitored over time. The compressive modulus was calculated by using the linear part of the curve between 10% and 20% compression.

**Cytotoxicity:** To assess cytotoxicity according to ISO 10993-5:2009 (Biological evaluation of medical devices, part 5: Tests for in vitro cytotoxicity), extracts were prepared and analyzed via MTT assay as previously described.<sup>[72]</sup> In brief, 200  $\mu\text{L}$  15% w/v 8armPEG10k-hydrogels were prepared for all linkers as described above. These hydrogels were incubated in 2 mL of EMEM supplemented with 10% FCS for 24 h at 37  $^{\circ}\text{C}$ . Afterward, extracts were prepared by separating the supernatant from the hydrogels. Meanwhile, mouse fibroblast L-929 cells were seeded in a 96-well microtiter plate at a density of 10 000 cells per well and cultivated overnight. 100  $\mu\text{L}$  extract was added to each well. 0.1% SDS was used as negative control and pure medium served as positive control. At least six replicates were prepared for each type of hydrogel. After 24 h of incubation at 37  $^{\circ}\text{C}$ , the medium was replaced with 200  $\mu\text{L}$  of a 1.5 mM MTT

solution. After 6 h of further incubation at 37  $^{\circ}\text{C}$ , the MTT solution was replaced with PBS containing 10% SDS, and the samples were incubated for 16 h at room temperature. Finally, the absorbance at 570 and 690 nm was measured using a FluoStar Omega microplate reader (BMG Labtech, Ortenberg, Germany). Cell viability was calculated by the difference in absorbance. The viability was normalized to the positive control. For best evidence, hydrogel formulations with the highest polymer concentration of 15% w/v were investigated. By using extracts, contact between hydrogels and cells was prevented, which could lead to a negative impact on the cells due to abrasion.

**Swelling and Degradation Studies:** Swelling and degradation studies were performed according to literature.<sup>[28]</sup> For all linkers, 8armPEG10k-hydrogels with polymer concentrations of 5%, 10%, and 15% w/v were prepared as described above. The hydrogels were weighed after cross-linking and transferred to LoBind Eppendorf tubes. 5 mL of a 50 mM phosphate buffer (pH 7.4) with 0.02% sodium azide was added and the hydrogels were incubated at 37  $^{\circ}\text{C}$  in a shaking water bath. At predetermined time points, the hydrogels were weighed and incubated in 5 mL of fresh buffer solution. Complete dissolution was achieved when no remaining material could be detected.

**Release of FITC-Dextran:** To assess the influence of the biodegradable linkers on the release kinetics, FITC-dextran was used as model substance. 2 mg of 150 kDa FITC-dextran was embedded in 200  $\mu\text{L}$  hydrogels with a polymer concentration of 15% w/v. To prepare a hydrogel containing FITC-dextran, the respective norbornene-functionalized precursor was dissolved in 100  $\mu\text{L}$  of a solution with a FITC-dextran concentration of 20  $\text{mg mL}^{-1}$ . To this mixture, 100  $\mu\text{L}$  of a solution containing 8armPEG10k-Tz with an equal molar amount of tetrazine to norbornene groups were added. Gelation was carried out for 1 h at 37  $^{\circ}\text{C}$ . The hydrogels were transferred into 5 mL LoBind Eppendorf tubes and incubated in 5 mL of 50 mM phosphate buffer (pH 7.4). The release experiments were performed in a shaking water bath at 37  $^{\circ}\text{C}$ . At regular time points, samples were withdrawn and replaced with fresh buffer. The samples were stored at 2–8  $^{\circ}\text{C}$  for further analysis. A FluoStar Omega fluorescence microplate reader (BMG Labtech, Ortenberg, Germany) was used to quantify the FITC-dextran concentration.

**Statistical Analysis:** All experiments were performed in triplicate, and the results are shown as mean  $\pm$  standard deviation. Statistical significance was assessed using one-way ANOVA. Post hoc analysis was determined by Tukey's test (GraphPad Prism 6.0, GraphPad Software Inc., La Jolla, CA).

## Supporting Information

Supporting Information is available from the Wiley Online Library or from the author.

## Acknowledgements

The authors thank Renate Liebl for technical assistance.  
Open access funding enabled and organized by Projekt DEAL.

## Conflict of Interest

The authors declare no conflict of interest.

## Data Availability Statement

Research data are not shared.

## Keywords

biodegradation, hydrogel, hydrolysis, Inverse electron demand Diels–Alder reaction, leaving group

Received: June 5, 2022  
Revised: August 29, 2022  
Published online: September 26, 2022

- [1] K. H. Bae, L.-S. Wang, M. Kurisawa, *J. Mater. Chem. B* **2013**, *1*, 5371.  
 [2] D. J. Overstreet, D. Dutta, S. E. Stabenfeldt, B. L. Vernon, *J. Polym. Sci., Part B: Polym. Phys.* **2012**, *50*, 881.  
 [3] J. D. Kretlow, L. Klouda, A. G. Mikos, *Adv. Drug Delivery Rev.* **2007**, *59*, 263.  
 [4] A. T. Metters, C. N. Bowman, K. S., *J. Phys. Chem. B* **2000**, *104*, 7043.  
 [5] X. Zhang, S. Malhotra, M. Molina, R. Haag, *Chem. Soc. Rev.* **2015**, *44*, 1948.  
 [6] S. Kirchhof, A. Strasser, H.-J. Wittmann Anseth, V. Messmann, N. Hammer, A. M. Goepferich, F. P. Brandl, *J. Mater. Chem. B* **2015**, *3*, 449.  
 [7] C. M. Madl, S. C. Heilshorn, *Chem. Mater.* **2019**, *31*, 8035.  
 [8] H. Tan, J. P. Rubin, K. G. Marra, *Macromol. Rapid Commun.* **2011**, *32*, 905.  
 [9] I. Altinbasak, R. Sanyal, A. Sanyal, *RSC Adv.* **2016**, *6*, 74757.  
 [10] C. E. Ziegler, M. Graf, S. Beck, A. M. Goepferich, *Eur. Polym. J.* **2021**, *147*, 110286.  
 [11] Z. Zhang, C. He, X. Chen, *Mater. Chem. Front.* **2018**, *2*, 1765.  
 [12] J. Kalia, R. T. Raines, *Angew. Chem., Int. Ed. Engl.* **2008**, *47*, 7523.  
 [13] H. Jiang, S. Qin, H. Dong, Q. Lei, X. Su, R. Zhuo, Z. Zhong, *Soft Matter* **2015**, *11*, 6029.  
 [14] Q. V. Nguyen, D. P. Huynh, J. H. Park, D. S. Lee, *Eur. Polym. J.* **2015**, *72*, 602.  
 [15] C.-C. Lin, A. T. Metters, *Pharm. Res.* **2006**, *23*, 614.  
 [16] Y. Liu, M. Liu, Y. Zhang, Y. Cao, R. Pei, *New J. Chem.* **2020**, *44*, 11420.  
 [17] S. T. Koshy, R. M. Desai, P. Joly, J. Li, R. K. Bagrodia, S. A. Lewin, N. S. Joshi, D. J. Mooney, *Adv. Healthcare Mater.* **2016**, *5*, 541.  
 [18] D. S. B. Anugrah, M. P. Patil, X. Li, C. M. Q. Le, K. Ramesh, G.-D. Kim, K. Hyun, K. T. Lim, *eXPRESS Polym. Lett.* **2020**, *14*, 248.  
 [19] A.-C. Knall, C. Slugovc, *Chem. Soc. Rev.* **2013**, *42*, 5131.  
 [20] W. Kang, B. Bi, R. Zhuo, X. Jiang, *Carbohydr. Polym.* **2017**, *160*, 18.  
 [21] Y. Hong, H. Song, Y. Gong, Z. Mao, C. Gao, J. Shen, *Acta Biomater.* **2007**, *3*, 23.  
 [22] W. E. Hennink, O. Franssen, W. N. E. Van Dijk-Wolthuis, H. Talsma, *J. Controlled Release* **1997**, *48*, 107.  
 [23] E. J. Oh, S.-W. Kang, B.-S. Kim, G. Jiang, I. H. Cho, S. K. Hahn, *J. Biomed. Mater. Res., Part A* **2008**, *86A*, 685.  
 [24] S. J. Buwalda, T. Vermonden, W. E. Hennink, *Biomacromolecules* **2017**, *18*, 316.  
 [25] M. Graf, C. E. Ziegler, M. Gregoritz, A. M. Goepferich, *Int. J. Pharm.* **2019**, *566*, 652.  
 [26] P. J. Levalley, R. Neelapapu, B. P. Sutherland, S. Dasgupta, C. J. Kloxin, A. M. Kloxin, *J. Am. Chem. Soc.* **2020**, *142*, 4671.  
 [27] W. N. E. Van Dijk-Wolthuis, J. A. M. Hoogeboom, M. J. Van Steenberg, S. K. Y. Tsang, W. E. Hennink, *Macromolecules* **1997**, *30*, 4639.  
 [28] F. Brandl, N. Hammer, T. Blunk, J. Tessmar, A. Goepferich, *Biomacromolecules* **2010**, *11*, 496.  
 [29] F. Van De Manakker, M. Van Der Pot, T. Vermonden, C. F. Van Nostrum, W. E. Hennink, *Macromolecules* **2008**, *41*, 1766.  
 [30] S. Kirchhof, F. P. Brandl, N. Hammer, A. M. Goepferich, *J. Mater. Chem. B* **2013**, *1*, 4855.  
 [31] C. E. Ziegler, M. Graf, M. Nagaoka, H. Lehr, A. M. Goepferich, *Biomacromolecules* **2021**, *22*, 3223.  
 [32] N. Hammer, F. P. Brandl, S. Kirchhof, A. M. Goepferich, *J. Controlled Release* **2014**, *183*, 67.  
 [33] A. K. Ghosh, M. Brindisi, *J. Med. Chem.* **2015**, *58*, 2895.  
 [34] D. Aydin, M. Arslan, A. Sanyal, R. Sanyal, *Bioconjugate Chem.* **2017**, *28*, 1443.  
 [35] M. Gregoritz, K. Abstiens, M. Graf, A. M. Goepferich, *Eur. J. Pharm. Biopharm.* **2018**, *127*, 194.  
 [36] J. Xu, E. Feng, J. Song, *J. Am. Chem. Soc.* **2014**, *136*, 4105.  
 [37] J. L. Dávila, M. A. D'ávila, M. A. d'Ávila, *Carbohydr. Polym.* **2017**, *157*, 1.  
 [38] W. F. Diller, *Toxicol. Ind. Health.* **1985**, *1*, 7.  
 [39] M. A. Mehlman, *Def. Sci. J.* **1987**, *37*, 269.  
 [40] T. M. O'shea, A. A. Aimetti, E. Kim, V. Yesilyurt, R. Langer, *Adv. Mater.* **2015**, *27*, 65.  
 [41] S. Kirchhof, M. Gregoritz, V. Messmann, N. Hammer, A. M. Goepferich, F. P. Brandl, *Eur. J. Pharm. Biopharm.* **2015**, *96*, 217.  
 [42] M. Gregoritz, V. Messmann, A. M. Goepferich, F. P. Brandl, *J. Mater. Chem. B* **2016**, *4*, 3398.  
 [43] M. R. Karver, R. Weissleder, S. A. Hilderbrand, *Bioconjugate Chem.* **2011**, *22*, 2263.  
 [44] A.-C. Albertsson, M. Eklund, *J. Appl. Polym. Sci.* **1995**, *57*, 87.  
 [45] I. Lee, C. K. Kim, B. C. Lee, *J. Comput. Chem.* **1987**, *8*, 794.  
 [46] C. M. Comisar, S. E. Hunter, A. Walton, P. E. Savage, *Ind. Eng. Chem. Res.* **2008**, *47*, 577.  
 [47] A. F. Hegarty, L. N. Frost, *J. Chem. Soc., Perkin Trans. 2* **1973**, <https://doi.org/10.1039/P29730001719>  
 [48] J. Hansen, N. Mørk, H. Bundgaard, *Int. J. Pharm.* **1992**, *81*, 253.  
 [49] X. Tong, S. Lee, L. Bararpour, F. Yang, *Macromol. Biosci.* **2015**, *15*, 1679.  
 [50] F. Brandl, F. Kastner, R. M. Gschwind, T. Blunk, J. Teßmar, A. Göpferich, *J. Controlled Release* **2010**, *142*, 221.  
 [51] J. Li, D. J. Mooney, *Nat. Rev. Mater.* **2016**, *1*, 16071.  
 [52] H. Wen, J. Hao, S. K. Li, *J. Pharm. Sci.* **2013**, *102*, 892.  
 [53] P. Kurtzhals, C. Larsen, M. Johansen, *J. Chromatogr., Biomed. Appl.* **1989**, *491*, 117.  
 [54] U. Bhardwaj, R. Sura, F. Papadimitrakopoulos, D. J. Burgess, *Int. J. Pharm.* **2010**, *384*, 78.  
 [55] Q. Peng, X. Sun, T. Gong, C.-Y. Wu, T. Zhang, J. Tan, Z.-R. Zhang, *Acta Biomater.* **2013**, *9*, 5063.  
 [56] V. Huynh, R. G. Wylie, *Angew. Chem., Int. Ed. Engl.* **2018**, *57*, 3406.  
 [57] K. W. Lee, J. J. Yoon, J. H. Lee, S. Y. Kim, H. J. Jung, S. J. Kim, J. W. Joh, H. H. Lee, D. S. Lee, S. K. Lee, *Transplant. Proc.* **2004**, *36*, 2464.  
 [58] K. Vulic, M. S. Shoichet, *J. Am. Chem. Soc.* **2012**, *134*, 882.  
 [59] K. Xu, F. Lee, S. Gao, M.-H. Tan, M. Kurisawa, *J. Controlled Release* **2015**, *216*, 47.  
 [60] D. A. Martin, S. Senanayake, *N. Engl. J. Med.* **2011**, *364*, 758.  
 [61] F. Brandl, M. Henke, S. Rothschenk, R. Gschwind, M. Breunig, T. Blunk, J. Tessmar, A. Göpferich, *Adv. Eng. Mater.* **2007**, *9*, 1141.  
 [62] O. A. Mukhina, D. M. Kuznetsov, T. M. Cowger, A. G. Kutateladze, *Angew. Chem., Int. Ed. Engl.* **2015**, *54*, 11516.  
 [63] O. A. Mukhina, N. N. Bhuvan Kumar, T. M. Arisco, R. A. Valiulin, G. A. Metzler, A. G. Kutateladze, *Angew. Chem., Int. Ed. Engl.* **2011**, *50*, 9423.  
 [64] N. Peppas, *Eur. J. Pharm. Biopharm.* **2000**, *50*, 27.  
 [65] P. J. Flory, *Principles of Polymer Chemistry*, 10th ed., Cornell Univ. Press, Ithaca, NY **1953**.  
 [66] J. C. Bray, E. W. Merrill, *J. Appl. Polym. Sci.* **1973**, *17*, 3779.  
 [67] D. L. Elbert, A. B. Pratt, M. P. Lutolf, S. Halstenberg, J. A. Hubbell, *J. Controlled Release* **2001**, *76*, 11.  
 [68] N. A. Peppas, E. W. Merrill, *J. Appl. Polym. Sci.* **1977**, *21*, 1763.  
 [69] E. Merrill, K. Dennison, C. Sung, *Biomaterials.* **1993**, *14*, 1117.  
 [70] T. Canal, N. A. Peppas, *J. Biomed. Mater. Res.* **1989**, *23*, 1183.  
 [71] G. P. Raebler, M. P. Lutolf, J. A. Hubbell, *Biophys. J.* **2005**, *89*, 1374.  
 [72] M. Gregoritz, V. Messmann, K. Abstiens, F. P. Brandl, A. M. Goepferich, *Biomacromolecules* **2017**, *18*, 2410.